Published in final edited form as:
Dev Cell. 2012 June 12; 22(6): 1191–1207. doi:10.1016/j.devcel.2012.04.018.

Fgf9 and FGF20 maintain the stemness of nephron progenitors in mice and man

Hila Barak[1,10], **Sung-Ho Huh**[1,10], **Shuang Chen**[1], **Cécile Jeanpierre**[3,4], **Jelena Martinovic**[5], **Mélanie Parisot**[3], **Christine Bole-Feysot**[6], **Patrick Nitschké**[7], **Rémi Salomon**[3,4,8], **Corinne Antignac**[3,4,9], **David M. Ornitz**[1,*], and **Raphael Kopan**[1,2,*]

[1]Department of Developmental Biology, Washington University School of Medicine, 660 South Euclid Ave., Campus Box 8103, St. Louis, MO 63110, USA

[2]Department of Medicine, Washington University School of Medicine, 660 South Euclid Ave., Campus Box 8103, St. Louis, MO 63110, USA

[3]Inserm, U983, Hôpital Necker, 75015 Paris, France

[4]Université Paris Descartes, Sorbonne Paris Cité, Institut Imagine, Paris, France

[5]Department of Fetopathology, Laboratoire Cerba, St Ouen-l'Aumône and AP-HP, Hôpital Antoine Beclere, Clamart, France

[6]Genomic Plateform, Fondation Imagine, Hôpital Necker-Enfants Malades, Paris, France

[7]Bioinformatic Plateform, Université Paris Descartes, Hôpital Necker-Enfants Malades, Paris, France

[8]AP-HP, Department of Pediatric Nephrology, Hôpital Necker-Enfants Malades, Paris France

[9]AP-HP, Department of Genetics, Hôpital Necker-Enfants Malades, Paris, France

Summary

The identity of niche signals necessary to maintain embryonic nephron progenitors is unclear. Here we provide evidence that Fgf20 and Fgf9, expressed in the niche, and Fgf9, secreted from the adjacent ureteric bud, are necessary and sufficient to maintain progenitor stemness. Reduction in the level of these redundant ligands in the mouse led to premature progenitor differentiation within the niche. Loss of FGF20 in humans, or of both ligands in mice, resulted in kidney agenesis. Sufficiency was shown in vitro where Fgf20 or Fgf9 (alone or together with Bmp7) maintained isolated metanephric mesenchyme or sorted nephron progenitors that remained competent to differentiate in response to Wnt signals after 5 or 2 days in culture, respectively. These findings identify a long sought-after critical component of the nephron stem cell niche and hold promise for long-term culture and utilization of these progenitors in vitro.

[*]Correspondence: dornitz@wustl.edu (D.M.O.), kopan@wustl.edu (R.K.).
[10]Equal contributions

Introduction

Different mammalian organs deploy different strategies to fulfill their physiological roles in the adult. The gut and the skin rely on stem cells sequestered in specialized niches to maintain homeostasis and recover from injury (Fuchs, 2008; Li and Clevers, 2010). In contrast, the adult kidney has no identifiable stem cells (Little and Bertram, 2009), displays limited repair capacity (Humphreys et al., 2008) and relies instead on a large surplus of nephrons generated from an embryonic pool of stem cells/progenitors during development. Genetic and environmental factors affect the number of nephrons; low numbers correlates with renal diseases and hypertension (Bertram et al., 2011; Keller et al., 2003; Myrie et al., 2011). Improved insight into the nephron progenitors and their environment may help maintain such cells for therapeutic purposes. Therefore, there is growing interest in understanding the mechanisms that regulate these cells during nephrogenesis.

Mammalian renal progenitors are established in the metanephric mesenchyme (MM) following ureteric bud (UB) outgrowth. The MM condenses around UB tips and induces tip branching (Costantini and Kopan, 2010); the distal aspect of the branched duct is a niche for embryonic multipotent stem/progenitor cells (Boyle et al., 2008; Kobayashi et al., 2008). Nephron progenitors located lateral or proximal to the UB tips form a pre-tubular aggregate (PTA) before undergoing mesenchymal to epithelial transition generating the renal vesicle (RV). The RV cells grow at different rates to form a S-shaped body (SSB). Nephron progenitors located distal to the UB form a “cap” and express the transcription factors *Six2* and *Sall1*, which play a critical role in maintaining stemness. *Six2*-deficient progenitors differentiate en masse prematurely in a Wnt9b-dependent manner (Kobayashi et al., 2008; Self et al., 2006), causing renal agenesis. The UB is thought to play a dual role. It makes an important contribution to maintaining progenitors capable of self-renewal and it provides Wnt9b that promotes differentiation of cap metanephric mesenchyme (CMM) (Carroll et al., 2005; Karner et al., 2011; Kobayashi et al., 2008; Park et al., 2007). This stem cell/progenitor population disappears after producing 1.5×10^6 (human) or 1.3×10^4 (mouse) nephrons, likely due to the disappearance of their niche (Hartman et al., 2007)

Whether niche signals maintain stemness or block differentiation is unclear. Paradoxically, Wnt9b may constitute part of the niche signal (Karner et al., 2011). However, a niche “stemness” signal, if one exists, is expected to specifically maintain self-renewal while keeping the cells competent to respond to differentiation signals by generating multiple lineages. Such a molecule would have therapeutic potential if it could be used to maintain and expand a population of multipotent renal stem cells in an artificial niche.

FGF ligands are among the candidates for the niche signal required to maintain stemness because inactivation of FGF receptors (*Fgfrs*) in the CMM results in arrested kidney development (Poladia et al., 2006; Sims-Lucas et al., 2011). Supporting the notion that FGF signals are essential for maintenance of the nephron progenitor population is the observation that supplementing isolated MM cells with FGF2 (which is not present in the CMM) and Bmp7 (which is) can maintain their competence in culture short-term (Dudley et al., 1999). Generally, FGF ligands expressed in mesenchymal tissues signal to epithelial splice forms of FGFRs (‘b’ splice forms), whereas ligands expressed in epithelial cells signal to mesenchymal splice forms of FGFRs (‘c’ splice forms; (Zhang et al., 2006)). Based on this, the ligand may be provided to the CMM by an epithelial source, (ie the UB). CMM cells express Fgf7 and Fgf10, which signal to epithelial Fgfr2b in the UB. Targeted deletion of *Fgf7* leads to a reduction in ureteric branch number due to decreased signaling through Fgfr2b and secondarily, to fewer nephrons (Bates, 2011; Qiao et al., 1999). *Fgf8*, expressed in the nascent RV, is required for progression from PTA to RV and for its proliferation (Grieshammer et al., 2005; Perantoni et al., 2005). Loss of *Fgf8* results in apoptosis of MM

due to loss of a PTA-derived signal, most likely Wnt4 (Grieshammer et al., 2005; Perantoni et al., 2005). Although these studies point to an important role for FGF signaling in maintaining the MM, the ligands that signal to mesenchymal Fgfrs *in vivo* have not been identified.

Here, we investigate the role of the *Fgf9* sub-family in renal development and discovered that Fgf9 acts redundantly with Fgf20 to promote the proliferation, survival and stemness of CMM progenitors *in vivo*. Moreover, we identified a human missense mutation in *FGF20* that results in bilateral renal agenesis. We show that either Fgf9 or Fgf20 were sufficient to maintain differentiation-competent, Six2+ nephron progenitors *in vitro* for 5 days, whereas cells grown in Fgf8 or Fgf10 lose competence by 48 hours. Sorted Six2+ cells retained competence to form epithelia for at least 48 hours in culture when grown in serum-free media containing Fgf9/BMP7. These studies identify Fgf20 (and Fgf9) as integral parts of the CMM niche where they act to maintain a self-renewing progenitor population competent to respond to an inductive cue. This work lays the foundation for creating an artificial renal stem cell niche.

Results

Fgf20 and Fgf9 act redundantly and are essential for kidney development

The *Fgf20* gene was targeted by insertion of a β-Galactosidase (βGal) cDNA into exon 1 (Huh et al., 2012). $Fgf20^{\beta Gal/\beta Gal}$ mice are viable, fertile and have a normal lifespan. They also display several phenotypes, including sensorineural hearing loss due to defects in the development of the organ of Corti (Huh et al., 2012). Examination of E18.5 kidneys from $Fgf20^{\beta Gal/\beta Gal}$ embryos revealed a reduction in kidney size (~15%) relative to control kidneys (n=8, P<0.03). Counts confirmed that fewer Glomeruli formed in $Fgf20^{\beta Gal/\beta Gal}$ and $Fgf20^{+/\beta Gal}$ kidneys relative to wild type (15684±3035 vs. 22350±2733; $p=8.1775\times10^{-8}$; 19392±3070 vs. 22350±2733, respectively; P=0.0028; Figure 1I). The adrenal glands, gonads and Wolffian duct of $Fgf20^{\beta Gal/\beta Gal}$ were indistinguishable from wild type, as was the gross histology of $Fgf20^{\beta Gal/\beta Gal}$ kidneys (Figure 1B; see also Figure 2 and 3). The intermediate steps in nephron development (formation of the RV, SSB and early glomeruli) were comparable to control (white line, Figure 1F-G', arrow SSB and arrowhead glomeruli). Thus, the overall smaller size was consistent with a smaller progenitor pool that differentiated normally.

Related FGFs have similar biochemical properties and developmental functions (Itoh and Ornitz, 2011; Zhang et al., 2006). We thus tested if the other members of the same subfamily (*Fgf9, Fgf16*) had redundant functions with Fgf20 in kidney development by generating compound *Fgf9* and *Fgf20* mutant animals. *Fgf20* compound heterozygous ($Fgf9^{+/-}$; $Fgf20^{+/\beta Gal}$ and $Fgf9^{-/-}$;$Fgf20^{+/\beta Gal}$) embryos did not exhibit any gross abnormalities (n=10 and 6, respectively; Figure 1C) *Fgf9*-deficient embryos display aberrant development of the male reproductive tract with no kidney abnormalities (Colvin et al., 2001a), and die after birth due to lung malformations (Colvin et al., 2001b); therefore, all subsequent analyses were conducted at E18.5 unless stated otherwise. In contrast, all $Fgf9^{+/-}$; $Fgf20^{\beta Gal/\beta Gal}$ embryos had hypoplastic kidneys (n=8). The defects ranged from mild (15% reduction in 8 kidneys, p= 0.005, Figure 1D') to severe (60% reduction in 6 kidneys, P<0.001, Figure 1D"). One embryo displayed bilateral renal agenesis (similar to Figure 1E). No defects were detected in the adrenal glands, gonads, Mullerian ducts, ductus deferens or bladder. Significantly, histological analysis revealed that in $Fgf9^{+/-}$; $Fgf20^{\beta Gal/\beta Gal}$ kidneys, large areas of the nephrogenic zone were missing, replaced by more mature tubular structures (Figure 1H-H', arrowheads). Kidney agenesis was observed in all $Fgf9^{-/-}$; $Fgf20^{\beta Gal/\beta Gal}$ embryos examined (n=6, Figure 1E, yellow arrowhead). In this genetic background, the adrenal glands were reduced in size (Figure 1E, white arrowhead).

These findings indicate that *Fgf9* and *Fgf20* function redundantly during kidney development to maintain the nephrogenic zone. Because one allele of *Fgf20* in *Fgf9* null embryos is enough to support normal kidney development, whereas $Fgf9^{+/-}; Fgf20^{\beta Gal/\beta Gal}$ mice display a severe phenotype, *Fgf20* seems to have a more dominant role than *Fgf9* in the kidney.

Reduction in *Fgf9* and *Fgf20* levels lead to loss of nephron progenitors and premature differentiation

To better characterize *Fgf9* and *Fgf20* deficient kidneys, we examined the expression of several molecular markers of nephron progenitors and their differentiated descendents in control, $Fgf20^{\beta Gal/\beta Gal}$ and $Fgf9^{+/-}; Fgf20^{\beta Gal/\beta Gal}$ dysplastic kidneys. The UB (Cytokeratin 8, Ck8) branched and formed a collecting duct in both control and mutant mice (Figure 2A-E). Wilms tumor 1 (WT1) was highly expressed in the podocytes, and Lotus Tetragonolobus Lectin (LTL) positive proximal convoluted tubules (PT) were readily detected. This and the fact that some $Fgf9^{+/-}; Fgf20^{\beta Gal/\beta Gal}$ mice survive to adulthood, confirmed the presence of mature, functional nephrons, albeit in reduced numbers within smaller, dysplastic kidneys (Figure 2A-E). Loss of Six2-positive CMM occurred in patches, consistent with an overall reduction in nephron progenitors (see below). As noted before, large areas in the nephrogenic zone of E18.5 $Fgf9^{+/-}; Fgf20^{\beta Gal/\beta Gal}$ kidneys were replaced by mature structures (Figure 2C,E, white arrows). Six2-expressing nephron progenitors also express Pax2 (paired-box homeotic transcription factor 2) and low levels of WT1 protein. These progenitors form one or two cell layers distal to each UB tip in both control ($Fgf20^{+/\beta Gal}$) and in most tips in $Fgf20^{\beta Gal/\beta Gal}$ kidneys (Figure 2A-A',D' yellow arrowheads) at E18.5. In contrast, in $Fgf9^{+/-}; Fgf20^{\beta Gal/\beta Gal}$ kidneys, three phenotypic categories can be discerned: normal CMM (Figure 2 yellow arrowheads), reduced progenitor numbers (Figure 2B', C', E' white arrowheads, also seen near a few tips in $Fgf20^{\beta Gal/\beta Gal}$ kidneys), or loss of progenitors leading to mature structures distal to UB tips (white arrows in Figure 2C-C',E').

To determine if these defects were intrinsic to the progenitors, we cultured E11.5 metanephroi of various genotypes for 2 days and stained for Ck8 and Six2. $Fgf20^{\beta Gal/\beta Gal}$ metanephroi were smaller than controls. To evaluate progenitor pool size, we counted the number of tips surrounded by Six2+ cells in each genotype (see experimental procedures for detail). Whereas UB tips in control animals were surrounded with Six2+ cells, 33.7% of $Fgf20^{\beta Gal/\beta Gal}$ UB tips were surrounded by fewer Six2+ cells (yellow arrows, Figure 3C) and 12.4% lacked Six2+ cells altogether (blue arrows, Figure 3c; quantification in M). $Fgf9^{+/-}; Fgf20^{\beta Gal/\beta Gal}$ metanephroi displayed a more severe phenotype (41% had fewer and 29.8% had no Six2+ cells; Figure 3D-F, M). Staining for the RV-SSB differentiation marker Jagged1 (Jag1) (Cheng et al., 2003; Cheng et al., 2007) detected numerous Jag1+ epithelial differentiating distal to the UB tip, where Six2-expressing mesenchyme should reside (Figure 3H-L, white arrows). Consistent with premature differentiation in the niche, *Wnt4* was ectopically expressed in cells surrounding UB tips in $Fgf9^{+/-}; Fgf20^{\beta Gal/\beta Gal}$ metanephroi (Figure 3K, white arrows). These observations are consistent with the hypothesis that Fgf9 and Fgf20 act to prevent premature differentiation of nephron progenitors, reminiscent of *Six2*-deficient mice (Self et al., 2006) or mice expressing constitutively active Notch in the CMM (Boyle et al., 2011; Cheng et al., 2007; Fujimura et al., 2010).

Fgf20 is expressed exclusively in nephron progenitors, whereas *Fgf9* signals mostly from the UB

To determine the temporal and spatial expression patterns of *Fgf20*, we analyzed FGF20-βGal activity during kidney development. Whole-mount X-gal staining at E10.5-12.5 clearly showed activity in mesonephric and metanephric kidneys (Figure 4A-C, black and red

arrowheads, respectively). At E14.5, βGal activity was present in the MM surrounding the UB (Figure 4D). To identify the specific cell population that expressed *Fgf20*, we stained sections of *Fgf20*$^{\beta Gal/\beta Gal}$ kidneys with antibodies against Ck8, Neural Cell Adhesion Molecule (NCAM, marking mesenchymal cells and their epithelial derivatives) and βGal. At E16.5, βGal co-localized with Six2 in CMM cells (Figure 4E-F, white arrows). βGal activity persisted in the nascent RV due to expression or perdurance (Figure 4E, yellow arrowhead) but not in the stroma or the UB (Figure 4E-F). We therefore conclude that in the metanephric kidney, *Fgf20* is expressed exclusively in nephron progenitors. This pattern agrees with the mRNA expression data collected by GUDMAP (Little et al., 2007) and presented in (Brown et al., 2011). The same resource describes *Fgf9* expression as most abundant in the UB, with MM expression detected P0-P2 (see Figure S1). mRNA for both ligands disappears as the remaining progenitors differentiate en-masse.

Conditional inactivation of *Fgfrs* in the CMM caused renal agenesis (Poladia et al., 2006), mimicked by *Fgf9/20* compound mutants (Figure 1). Because *Fgf9* is expressed in the duct (Barasch et al., 1997; Brown et al., 2011; McMahon et al., 2008), we hypothesized that Fgf9 is a paracrine signal from the duct to the CMM and FGF20 acts in an autocrine manner on the CMM itself. To test this, we inactivated a conditional allele of *Fgf9* (*Fgf9*$^{f/f}$; (Lin et al., 2006)) specifically in the UB, with the *HoxB7-Cre* BAC transgene (Yu et al., 2002). Removal of both *Fgf9* alleles from the UB in *Fgf20*$^{+/\beta Gal}$ embryos permitted normal development (Figure 4G-H,K-K'). Conversely, when a single allele of *Fgf9* was removed from the UB of *Fgf20*$^{\beta Gal/\beta Gal}$ embryos (*HoxB7-Cre*$^{+/tg}$*; Fgf9*$^{+/f}$*; Fgf20*$^{\beta Gal/\beta Gal}$), dysplastic, smaller kidneys formed (25-75%; n=10; Figure 4I). Examination of these kidneys (Figure 4L-L') revealed depletion of nephron progenitors similar to that seen with global loss of an *Fgf9* in this background (Figure 2). *Fgf20* null embryos lacking both *Fgf9* alleles in the UB (*HoxB7-cre*$^{+/tg}$*; Fgf9*$^{f/f}$*; Fgf20*$^{\beta Gal/\beta Gal}$) displayed rudimentary kidneys (n=6) or renal agenesis (n=4) (Figure 4J), a phenotype slightly milder than the *Fgf9*/Fgf20 compound null. To ask if Fgf9 was expressed in the MM, we deleted *Fgf9* from the mesenchyme using the *Pax3-Cre* allele (Cheng et al., 2007; Li et al., 2000). Some *Pax3-Cre*$^{+/tg}$*; Fgf9*$^{f/f}$*; Fgf20*$^{\beta Gal/\beta Gal}$ mice have rudimentary kidneys (Figure S1), consistent with *Fgf9* being expressed in the mesenchyme. These data support a model in which Fgf9 secreted from the UB complements the activity of Fgf20 and Fgf9 produced in the CMM.

FGF20 loss is associated with renal agenesis in human

Independently, we used a combined approach of homozygosity mapping and exome sequencing to analyze a consanguineous family with several fetuses presenting with isolated bilateral renal agenesis. Autopsy revealed the Potter sequence and bilateral reno-ureteral agenesis (Figure 5A) in one fetus. Other organs were normal. DNA analysis from this fetus identified homozygous variants in four genes expressed during early kidney development and located in homozygous chromosomal regions. One of these mutations was a single base-pair deletion in exon 2 of *FGF20*, resulting in a frameshift starting at amino acid 113 and terminating in a stop codon at position 121, before the third Heparin-binding domain of the protein (Figure 5B-D, mutations (c.337delG)). Sanger sequencing analysis confirmed homozygosity for the *FGF20* c.337delG mutation in this fetus. Moreover, we showed that the mutation was homozygous in two other affected fetuses in the family and heterozygous in the parents with available DNA (Figure 5B). This mutation was absent in a healthy sibling (Figure 5B), from dbSNP and the 1000 genome database, and was not found in our in-house whole exome sequence data. Moreover, the three other homozygous variants identified in this fetus did not segregate with the kidney defect in this family. Combined with the mouse mutants described above, these data point to FGF20 as an essential protein during mammalian metanephric kidney development whose loss is sufficient to cause bilateral renal agenesis in humans.

In the absence of *Fgf9* and *Fgf20*, nephron progenitors form but are not maintained

Renal epithelia fail to form in humans lacking *FGF20* or in mice lacking *Fgf9* and *Fgf20*. We next asked if kidney agenesis reflected failure to establish the CMM (Costantini and Kopan, 2010) or failure to maintain the progenitors. Since the CMM induces UB outgrowth, we asked if UB induction was initiated properly in mutants by whole-mount Ck8 staining. By E11.5, control embryos had an elongated, T-shaped UB (Figure 6A). $Fgf9^{-/-}; Fgf20^{\beta Gal/\beta Gal}$ embryos initiated UB outgrowth, but in contrast, we only observed a branched UB in 2 out of 7 embryos (Figure 6B). To examine the MM, transverse sections of E11.5 embryos were prepared. In all embryos, the elongating UB contacted the Pax2-positve MM (Figure 6C-H). Control MM cells condensed around the UB in wild type embryos (Figure 6C), whereas the $Fgf9^{-/-}; Fgf20^{\beta Gal/\beta Gal}$ MM was significantly smaller and most cells failed to coalesce around the UB (Figure 6D). TUNEL staining detected many apoptotic cells within the MM of $Fgf9^{-/-}; Fgf20^{\beta Gal/\beta Gal}$ embryos at E11.5 (Figure 6E-F). By E12.5, only a few Pax2+, Ck8− cells remained in the mesenchyme (Figure 6G-H). This analysis suggested that, in the absence of *Fgf9* and *Fgf20*, UB outgrowth was initiated, but the rudimentary MM failed to migrate towards the UB and, in addition to prematurely differentiating (Figure 3 L-K), underwent high rates of apoptosis reminiscent of isolated MM cells *in vitro* and of *Fgfr*-deficient MM *in vivo* (Poladia et al., 2006). Analysis of *Pax2* and *Gdnf* expression in the MM correlated to the dose of *Fgf9/20* as early as E10.5-11.5. In contrast, *Pax2* (Figure 6) and *cRet* expression (data not shown) in the UB was unchanged. It cannot be ruled out that Fgf9 has a function in maintaining Etv4 and Etv5 in the UB epithelium (data not shown). The consequence of reduction in GDNF/ret signaling was progressive failure in branching morphogenesis (data not shown), which could be reversed *in vitro* by the addition of GDNF to metanephroi with limited branching (Figure S2).

Fgf9 maintain isolated progenitors competent to respond to inductive signals *in vitro*

The data presented thus far shows that Fgf20 and Fgf9 together are required for maintenance and survival of nephron progenitors in mice, and infer a similar activity for FGF20 in humans. Moreover, our allelic series indicates that stemness and survival were sensitive to the dose of *Fgf9/20* (predicting reduced nephron numbers in humans heterozygous for *FGF20*). To test if these ligands were sufficient to mimic the niche, we examined the ability of recombinant FGF9 to preserve the stemness of isolated nephron progenitors *in vitro*. MM was isolated from E11.5 kidneys and explants were grown in serum free media supplemented with Heparin (an important cofactor for FGF signaling; (Yayon et al., 1991)), or Heparin plus FGF9. In this and subsequent experiments, the absence of UB was confirmed by Ck8 staining. To assess survival, we used TUNEL staining; to identify mitotic cells, we used anti phospho-histone H3 (pHH3) antibody. As reported, the majority of isolated MM cells were TUNEL-positive after 4 days in media (Figure 7A). When Heparin was added, a greater number of cells survived and some mitotic cells were seen (Figure 7B). The addition of FGF9 and Heparin improved both survival and proliferation (Figure 7C). Anti-Cited1, Wt1 (not shown) and Six2 antibody staining 48hr after MM isolation confirmed that these markers were maintained in explants cultured in Heparin/FGF9-containing media (Figures 7E-E'), but not with Heparin alone. Some Six2-expressing cells were mitotic (Six2+; pHH3+; Figure 7F-I). These data demonstrate that the addition of FGF9 was sufficient to promote survival and support proliferation of some nephron progenitors *in-vitro*.

Next we asked whether nephron progenitors grown in the presence of FGF9 retained their competence to respond to inductive signals. To avoid introduction of renal tissue, we used freshly dissected dorsal spinal cord segments (dSC; (Saxen and Lehtonen, 1987; Saxen and Sariola, 1987)) as a source of Wnt (Herzlinger et al., 1994; Kispert et al., 1998). After 48hrs in Heparin/FGF9 media, dSC was added and the cells were maintained for an additional 2-4

days in serum free media. All freshly isolated control MM grown in contact with the dSC underwent MET (data not shown). After two days *in vitro*, only FGF9-supplemented MM differentiated into epithelia expressing either early distal (Cdh1) or proximal (Jag1) markers and retaining a few Six2+ progenitors (Figure 7J-K). The fact that these tubular structures contained at least two differentiated cell types (distal and proximal epithelial cells) strongly suggests that progenitor multipotency was retained.

It is clear that Fgf20 plays a more dominant role than Fgf9 *in vivo* and that any other Fgfs present in the cortex during development (Fgf2, Fgf8 and Fgf10) cannot rescue the niche in the absence of *Fgf9* and *Fgf20*. Fgf9 and Fgf20 share biochemical properties that may be unique among Fgf ligands expressed in the vicinity of the niche. To test this possibility, we cultured isolated E11.5 MM for 48hrs in Heparin supplemented media and added FGF9, FGF20, FGF8 or FGF10. First, we established the activity of our recombinant proteins on FGFR2b and FGFR2c splice variants stably expressed in Baf3 cells (Ornitz et al., 1996) Very few Six2-expressing cells (~10 cells/explants) were seen in the presence of FGF8 (7/7 explants); none were detected in eight explants exposed to FGF10 (Figure S3). In summary, these data demonstrated that members of the Fgf9/20 sub-family are necessary and sufficient to promote survival, competence and multipotency of MM cells *in vitro*.

Bmp7 synergizes with Fgf9 to promote survival and competence of nephron progenitors *in vitro*

FGF2 and BMP7 synergized to improve maintenance of nephron progenitors *in vitro* (Dudley et al., 1999). To test if BMP7 can enhance the effect of the endogenous niche ligand, we cultured isolated MM in media supplemented with BMP7 and FGF9. Whereas isolated MM supplemented with BMP7 alone lost their Six2+ population (Figure 8A), BMP7/FGF9 seemed to increase the overall number of Six2+ cells and induced nephron progenitors to sort away from Six2− cells and aggregate, confounding efforts to count them (Figure 8B-B'). In the presence of dSC, numerous epithelial structures containing distal (Cdh1+) and proximal (Jag1+) cells formed, each surrounded by a tight cluster of Six2+ cells (Figure 8C-D). To assess for self-renewal of nephron progenitors in media supplemented with BMP7 and FGF9, EdU (5-ethynyl-2'-deoxyuridine) was added to freshly isolated MM for 4-7hr, washed and refed the cells every 12hrs. After two days many Six2+ cells that remained EdU^{bright} (Figure 8E-H, yellow arrows) were detected, suggesting that they only divided once. A few Six2+, EdU^{Dimm} cells (progenitors that divided once after labeling or labeled late in S phase) were in mitosis after 48hrs (stained by pHH3, Figure 8E-H, turquoise arrow). Since mammalian S, G2 and M phases are relatively fixed in length, such double label indicates that some nephron progenitors were able to divide twice (one immediately after culture, the other two days later) in the presence of BMP7 and FGF9.

To ask if Six2+ cells could be maintained for as long as they live *in vivo* (from E11.5 to P2, or 8 to 10 days), we cultured isolated MM with FGF9 and BGF7 for 8 days in culture. Notably, although some Six2 expressing cells were in mitosis (Six2+; pHH3+; Figure S4 A-C, yellow arrows), the proportion of Six2+ cells declined after 5 days in these conditions (Figure 8 I, I'); by day 8, only a few Six2+ cells were detectable (data not shown). Staining for differentiation markers after 5 days confirmed that no Cdh1 or Cdh6 expressing epithelia formed in the absence of inducers (data not shown). Importantly, after 5 days in Heparin/FGF9/BMP7 media *in vitro*, Six2+ nephron progenitors formed epithelial tubules when co-cultured with dSC for an additional 4 days in basal media (9/9, three individual MM each in three repeats). These epithelia expressed either proximal (Cdh6) or distal (Cdh1) markers (Figure 8J).

Finally, to determine if FGF9 acted directly on Six2+ cells or indirectly through FoxD1+ stromal cells, we sorted GFP+ cells by FACS from *Six2-GFP::CRE*$^{tg/+}$ kidneys. Small

colonies of Six2+ cells, maintained for 48hrs in serum free media supplemented with FGF9, remained competent to differentiate (Figure 7L). Culturing these cells with FGF9+BMP7 for 48hr resulted in robust expansion of many more Six2+ colonies (Figure 8K-K') that maintained competence to respond to differentiation signals and produced epithelia expressing either proximal (Cdh6) or distal (Cdh1) markers after co-culture with dSC (Figure 8L). Mitotically active nephron progenitors (Six2+; pHH3+) survived after 5 days (Figure S4E-F, yellow arrows). Although when cultured with dSC they could form a few Cdh1 or Cdh6 positive cells, tubular epithelia no longer formed (data not shown). These data demonstrate that Fgf9/Bmp7 act directly on progenitors, promoting their survival while maintaining their competence to respond to inductive signals for at least 2 days.

Discussion

Here we present data demonstrating that members of the Fgf9 ligand family are bona fide secreted niche signals in the developing mammalian kidney. FGF20 acts alone in humans but is redundant with Fgf9 in mouse. In the absence of Fgf9 and Fgf20, UB outgrowth initiates, but because the MM undergoes a high rate of apoptosis, or because Fgf9 signals needed to maintain Etv4 and Etv5, UB branching is halted and kidney development fails. In human fetuses homozygous for a truncated allele of *FGF20*, no kidneys form. In mice, a single allele of *Fgf20* (*Fgf9*$^{-/-}$; *Fgf20*$^{+/\beta Gal}$) is sufficient to maintain normal kidney development *in vivo* (however, not in isolated MM), whereas a single allele of *Fgf9* (*Fgf9*$^{+/-}$; *Fgf20*$^{\beta Gal/\beta Gal}$) is insufficient. The redundancy between Fgf9 and Fgf20 produced highly informative variable phenotypes ranging from near normal kidneys to renal agenesis. When Fgf9 and Fgf20 are at limiting doses, the balance between differentiation and self-renewal is disturbed, Six2 expression is reduced, and precocious CMM differentiation can occur suggesting a role for FGF signaling in the maintenance of nuclear factors necessary for stemness (Osafune et al., 2006; Sakaki-Yumoto et al., 2006; Self et al., 2006). Consequently, many *Fgf9*$^{+/-}$; *Fgf20*$^{\beta Gal/\beta Gal}$ kidneys contain regions where nephron progenitors were replaced by differentiating epithelia, reminiscent of MM lacking *Six2* (Kobayashi et al., 2008; Self et al., 2006). Members of the Fgf9 sub-family are unique in that they can signal to both 'b' and 'c' splice forms of some Fgfr (Figure S3E and (Ornitz et al., 1996; Zhang et al., 2006)). However, autocrine Fgf9 also regulates epithelial growth and branching (del Moral et al., 2006; White et al., 2006; Yin et al., 2011; Yin et al., 2008). Although genetic deletion confirmed that mesenchymal Fgf9 makes a measurable contribution to the niche, the bulk of Fgf9 signals are provided from the epithelia (UB) to mesenchyme (MM). In contrast, Fgf20 was expressed exclusively in the CMM, signaling in an unusual autocrine fashion to maintain the mesenchymal cells in which it is expressed. Interestingly, in the developing organ of Corti, Fgf20 provides an autocrine signal acting within the epithelium to regulate its differentiation (Huh et al., 2012).

Independently, other investigators observed that Bmp7, expressed in nephron progenitors, UB and PTA during early kidney development (Dudley et al., 1995), acts to promote survival and proliferation of nephron progenitors (Blank et al., 2009; Dudley et al., 1999; Dudley et al., 1995; Dudley and Robertson, 1997; Godin et al., 1998). In *Bmp7* null mice, the first round of nephrogenesis is induced, followed later by loss of nephron progenitors, resulting in premature termination of kidney development (Dudley et al., 1995). Moreover, Fgf2, which like Fgf9 is expressed in the UB, can promote survival and maintain competent MM cells *in vitro* (Barasch et al., 1997; Dudley et al., 1999; Perantoni et al., 1995). However, FGF2 is not necessary in the niche as *Fgf2* null mice do not display a kidney phenotype (Zhou et al., 1998). FGF2, FGF8 and FGF10 could not rescue *Fgf9/20* null embryos, indicating that their function does not overlap with Fgf9/20 during kidney development. FGF7 and FGF10 signal to the UB and can replace GDNF when the inhibitor *Sprouty1* is removed (Michos et al., 2010). Fgf8 is expressed in the RV and in renal

epithelia and is needed for their maintenance (Grieshammer et al., 2005; Perantoni et al., 2005). *In vitro* analysis confirmed that FGF8 and FGF10 cannot maintain isolated MM, perhaps due to higher affinity of Fgf8 to the decoy receptor Fgfrl1, which is expressed in CMM (Brown et al., 2011). Moreover, several other ligands capable of activating the PI3K pathway can act as well as Fgf9 in maintenance of the progenitors (Brown et al., 2011), but our *in vivo* analysis demonstrates that none can rescue the loss of Fgf20 and Fgf9.

In contrast to Fgf8, either Fgf9 or Fgf20 are sufficient to support a Six2+ cell population that remained competent to respond to dSC by differentiating into different cell types. FGF9 maintains sorted, purified progenitors for at least 5 days; this is only possible if Fgf9 acted directly on the progenitors and rules out an indirect role via an essential, Fg9-dependent UB or stromal factor. Although restoring the unique cohesion of CMM cells *in vitro* also requires Bmp7, this cohesion is not needed for retention of competence; Fgf9 alone was sufficient to maintain Six2+ progenitors that are competent to differentiate in response to Wnt. Nonetheless, Bmp7 helps to organize cells into a structure that resembles the CMM niche, perhaps maximizing the benefits of endogenous Fgf20. At present, it is unclear if conditions that allow robust growth rates are compatible with maintaining competence as highly proliferative Six2+ cells in nephrospheres lost their competence to differentiate (Lusis et al., 2010).

It is thought that Wnt9b signals maintain stemness where Six2 is present and drives differentiation where Six2 is absent (Carroll et al., 2005; Karner et al., 2011; Kobayashi et al., 2008; Self et al., 2006). Although it is clear that self-renewing nephron progenitors receive a Wnt9b signal within the CMM (Karner et al., 2011), it is also evident that in the absence of Wnt9b, nephron progenitors survive; they do not undergo apoptosis, and they remain competent to respond to inductive signals as late as E13.5 (Karner et al., 2011)). These observations indicate that signals other than Wnt9b maintain competent nephron progenitors in *Wnt9b* mutant mice, and that in the absence of Wnt9b, proliferation is attenuated and differentiation is lost. Fgf9 and Fgf20 could provide this signal; both are Wnt-responsive genes in some contexts (Chamorro et al., 2005; Karner et al., 2011). The details of the relationships between Wnts and FGFs within the MM remain to be elucidated.

In conclusion, these observations suggest that, at a minimum, Fgf9/20 and Bmp7 organize the nephron progenitor niche and highlight the essential role of FGF20 in human kidney development. Regulating the balance between self-renewal and differentiation is key in determining nephron number, and lower nephron numbers are correlated with higher risk for hypertension, kidney disease, and recovery from injury. Our data indicate that FGF signaling likely regulates multiple important steps in the niche, including survival, proliferation, and competence. The relative contribution of each of these to maintenance of a proper niche is unclear. Since nephron progenitors do not persist in the adult, understanding the mechanisms that regulate this niche is a key step in the development of new therapeutic cell-replacement approaches. The identification of the endogenous niche ligands (Fgf9 and Fgf20) and the demonstration that they can maintain purified progenitors for 5 days *in vitro* opens the possibility for long-term maintenance of self-renewing nephron progenitors in culture. The importance of such a culture for research is self-evident; the therapeutic potential of these cells will have to be empirically determined in various injury models.

Experimental Procedures

Mice

All mice were maintained in the Washington University animal facility according to animal care regulations; Animals Studies Committee of Washington University approved the experimental protocols (protocol number 20110027). Lines used here are: *Fgf20*$^{\beta Gal}$ (Huh et

al., 2012); *Fgf9*$^{-}$ (Colvin et al., 2001a); *Fgf9*^{f} (Lin et al., 2006); *HoxB7-Cre*$^{+/tg}$ (Yu et al., 2002) and *Six2-GFP::CRE*$^{tg/+}$ (Park et al., 2007). Mice and embryos were genotyped using the universal PCR genotyping protocol (Stratman et al., 2003). Primers sequences available upon request.

Organ culture

Isolation and culture of metanephric kidneys were performed as described (Barak and Boyle, 2011). To manually isolate the MM, E11.5 metanephric kidneys were dissected in cold PBS. Kidneys were treated with 2.25% pancreatin and 0.75% trypsin in Ca-Mg free Tyrode's solution (pH7.4) (P/T solution) for 30s, then washed with FBS. MM was dissected from the UB using 26G needles and placed on transwell filters. Explants were cultured at 37°C, 5% CO_2 in defined medium (Barak and Boyle, 2011) supplemented with the following as indicated. 1μg/ml Heparin (Sigma), 8.6nM FGF9 (PeproTech), 50ng/ml BMP7 (R&D systems) and 100ng/ml FGF2 (PeproTech for positive control, data not shown). FBS was added as carrier in stock solutions (same results were obtained with BSA as carrier). Media was changed daily and activity of FGFs protein was tested by a Baf3 assay as described (Ornitz et al., 1996). To examine competence to respond to inductive signal, dSC was isolated from E11.5-13.5 embryos. Two fresh dSC segments were placed adjacent to each MM explant. Explants were then cultured for an additional 2-4 days in unsupplemented media. At least 3 explants per treatment were prepared for each experiment. Experiments were repeated at least 3 times on different days. Staining for Ck8 was performed to confirm exclusion of UB remnants from explants.

Six2+ cell sorting

Kidneys were dissected from E14.5-E17.5 embryos from wild type females mated with *Six2-GFP::CRE*$^{tg/+}$ males. Both GFP positive and negative kidneys were collected, with negative kidneys serving as sorting controls. To dissociate the cells into single cell suspension, kidneys were treated with pancreatin/trypsin diluted in Tyrode s solution (Ca^{+2}, Mg^{+2} free) for 15min on ice (200ul per 4-8 kidneys), followed by pipetting until clumps were not visible. To stop digestion, 1ml of cold DMEM with 10% FBS was added to the 200ul of enzyme solution. Cell suspension was then filtered through a 50μm filter (CellTrics®-Partec disposable filters 04-004-2327), collected in 1.5ml tubes and centrifuged for 4min at 800rpm. Media was aspirated and cells were resuspended in FACS buffer (3% FCS in PBS). GFP+ cells were sorted using a MoFlo high-speed flow cytometer (Dako Cytomation, Fort Collins, CO). Gating was implemented based on negative control profiles to select for live GFP positive cells. Sorted cells were collected in 1.5ml tubes (50,000-100,000 cells per tube) containing kidney media with 5% FBS and kept on ice before plating. Finally, cells were spun down for 4min at 800rpm and plated directly on transwell filters in organ culture dishes with kidney media supplemented with Heparin containing Fgf9 or Fgf9 and Bmp7. Media was changed every 12hr.

Immunohistochemistry

Immunohistochemistry was performed as detailed in supplemental data.

Statistical analysis and imaging

Two-tailed unpaired t-tests were performed for statistical analysis. Resulting *p* values are noted in text. For comparaison of kidney sizes, perimeter was measured and used for statistical analysis. Images were acquired with a Zeiss Axioimage Z1 equipped with an ApoTome or with stereomicroscope Leica MZ10F.

Quantification of nephron numbers—Kidneys were dissected from P5 pups of Fgf20 WT (+/+), Fgf20 +/βgal (+/-) and Fgf20 βgal/βgal (-/-) mice. To dissociate the tissue, kidneys were chopped into $2mm^2$ pieces and digested in 5ml of 6N HCL at 37°C for 90min. Tissue was further dissociated by repeated pipetting. 25ml of ddH2O was added to each sample, and samples were kept at 4°C. To count the number of nephrons, 100μl of well-mixed suspension was placed onto a 1cm×1cm area in a p100 culture dish marked with gridlines. The number of glomeruli were counted under an inverted microscope 5 times. Total number of glomeruli was estimated as follows: Total nephron number per pair of kidneys= average number of glomeruli in 100ul × 300.

Patients and whole exome sequencing

The fetus studied by exome sequencing (fetus 2 in Figure 5B) was an 18-week gestation male terminated for recurrence of bilateral renal agenesis with anhydramnios. The couple was consanguineous (first cousins) Caucasian; the mother was a healthy 25-year-old woman with previous history of termination of pregnancy at 26 weeks for anhydramnios. In this family, another consanguineous couple also experienced two terminations of pregnancy for bilateral renal agenesis (fetuses 3 and 4 in Figure 5B). At autopsy, fetus 2 was eutrophic, presented the Potter sequence including redundant skin, varus feet and pulmonary hypoplasia. Internal examination showed bilateral reno-ureteral agenesis (Figure 5A). Other organs were normal. X-ray evaluation showed no anomaly for the gestational age. Neuropathological examination did not detect any abnormality in brain or eyes. DNA was extracted from a frozen liver sample of fetus 2. Genotyping was performed on Illumina Infinium HumanOmni1 beadchip, resulting in the identification of 26 homozygous genomic regions extending from 35 Mb to 700 Kb and spanning the genome (data not shown). Whole exome sequencing was performed using the 50 Mb Agilent SureSelect assay and a SOLiD4 sequencer (50 base fragment reads). The 1.4 Gb of mappable sequence data were aligned to the human genome reference sequence (hg19 build) using BWA aligner (Li and Durbin, 2010). Variants were annotated with in house pipeline based on the Ensembl database (release 61). Known variants from dbSNP132, the 1000 Genomes Project and in-house exome data were excluded from the genetic variants identified in the coding regions or splice sites. Subsequent filtration of the data was performed in order to select variants located in the identified homozygous genomic regions, in genes expressed in the early stages of kidney development (http://www.gudmap.org/) and with a predicted deleterious effect on the protein (Polyphen, Sift). Mutations identified by exome sequencing were validated by Sanger sequencing in all available DNA samples of the family: fetus 2, his parents, a healthy sister and fetuses 3 and 4. The study was approved by the Comité de Protection des Personnes pour la Recherche Biomédicale Ile de France 2 and informed consent was obtained from the parents.

Supplementary Material

Refer to Web version on PubMed Central for supplementary material.

Acknowledgments

We thank the family with renal agenesis for their participation in the study. We wish to thank Drs. Fen Wang (*Fgf9*$^{f/f}$ mice), Andrew McMahon (Six2 antibody, *Six2-GFP::Cre* and *HoxB7-Cre* mice), Frank Costantini, Masato Hoshi, Sanjay Jain and Gail Martin for sharing reagents and transgenic animals; Scott Boyle, Kamesh Surenduran, Chihiro Sato and Courtney Karner for discussions and critical reading of the manuscript; Ling Li for assistance with FGF activity assays; Tao Shen and Hannah Weis for assistance with animal husbandry and mouse genotyping; Mary Fulbright for expert technical help; and the Department of Developmental Biology Histology Core for preparation of tissue sections. We thank William Eades, Christopher Holley and Jacqueline Hughes at the Siteman Cancer Center High Speed Sorter Core Facility for performing cell-sorting; Jeanne Amiel for providing DNA from two fetuses; Wassila Carpentier for genotyping analysis; and Solenn Pruvost and Mohamed Zarhrate for technical

assistance. RK, SC and HB were supported by a grant from the National Institutes of Diabetes and Digestive and Kidney Disease (DK066408) and the O'Brien Center Grant (5P30DK079333 to HB) provided support for organ culture experiments. The Siteman Cancer Center is supported in part by NCI Cancer Center Support Grant P30 CA91842. This work was supported in part also by a grant from the March of Dimes (DMO) and NIH support grants, P30DC04665, P30DK052574 and P30AR057235, for production of mice. Human sequencing analysis was supported by the GIS-Institut des Maladies Rares program (AAE11010KSA to CJ).

References

Barak H, Boyle SC. Organ culture and immunostaining of mouse embryonic kidneys. Cold Spring Harb Protoc 2011. 2011 pdb prot5558.

Barasch J, Qiao J, McWilliams G, Chen D, Oliver JA, Herzlinger D. Ureteric bud cells secrete multiple factors, including bFGF, which rescue renal progenitors from apoptosis. Am J Physiol. 1997; 273:F757–767. [PubMed: 9374839]

Bates CM. Role of fibroblast growth factor receptor signaling in kidney development. Pediatr Nephrol. 2011

Bertram JF, Douglas-Denton RN, Diouf B, Hughson MD, Hoy WE. Human nephron number: implications for health and disease. Pediatr Nephrol. 2011; 26:1529–1533. [PubMed: 21604189]

Blank U, Brown A, Adams DC, Karolak MJ, Oxburgh L. BMP7 promotes proliferation of nephron progenitor cells via a JNK-dependent mechanism. Development. 2009; 136:3557–3566. [PubMed: 19793891]

Boyle S, Misfeldt A, Chandler KJ, Deal KK, Southard-Smith EM, Mortlock DP, Baldwin HS, de Caestecker M. Fate mapping using Cited1-CreERT2 mice demonstrates that the cap mesenchyme contains self-renewing progenitor cells and gives rise exclusively to nephronic epithelia. Dev Biol. 2008; 313:234–245. [PubMed: 18061157]

Boyle SC, Kim M, Valerius MT, McMahon AP, Kopan R. Notch pathway activation can replace the requirement for Wnt4 and Wnt9b in mesenchymal-to-epithelial transition of nephron stem cells. Development. 2011; 138:4245–4254. [PubMed: 21852398]

Brown AC, Adams D, de Caestecker M, Yang X, Friesel R, Oxburgh L. FGF/EGF signaling regulates the renewal of early nephron progenitors during embryonic development. Development. 2011; 138:5099–5112. [PubMed: 22031548]

Carroll TJ, Park JS, Hayashi S, Majumdar A, McMahon AP. Wnt9b plays a central role in the regulation of mesenchymal to epithelial transitions underlying organogenesis of the mammalian urogenital system. Dev Cell. 2005; 9:283–292. [PubMed: 16054034]

Chamorro MN, Schwartz DR, Vonica A, Brivanlou AH, Cho KR, Varmus HE. FGF-20 and DKK1 are transcriptional targets of beta-catenin and FGF-20 is implicated in cancer and development. Embo J. 2005; 24:73–84. [PubMed: 15592430]

Cheng H, Miner J, Lin M, Tansey MG, Roth KA, Kopan R. g-Secretase Activity is Dispensable for the Mesenchyme-to-Epithelium Transition but Required for Proximal Tubule Formation in Developing Mouse Kidney. Development. 2003; 130:5031–5041. [PubMed: 12952904]

Cheng HT, Kim M, Valerius MT, Surendran K, Schuster-Gossler K, Gossler A, McMahon AP, Kopan R. Notch2, but not Notch1, is required for proximal fate acquisition in the mammalian nephron. Development. 2007; 134:801–811. [PubMed: 17229764]

Colvin JS, Green RP, Schmahl J, Capel B, Ornitz DM. Male-to-female sex reversal in mice lacking fibroblast growth factor 9. Cell. 2001a; 104:875–889. [PubMed: 11290325]

Colvin JS, White AC, Pratt SJ, Ornitz DM. Lung hypoplasia and neonatal death in Fgf9-null mice identify this gene as an essential regulator of lung mesenchyme. Development. 2001b; 128:2095–2106. [PubMed: 11493531]

Costantini F, Kopan R. Patterning a complex organ: branching morphogenesis and nephron segmentation in kidney development. Dev Cell. 2010; 18:698–712. [PubMed: 20493806]

del Moral PM, De Langhe SP, Sala FG, Veltmaat JM, Tefft D, Wang K, Warburton D, Bellusci S. Differential role of FGF9 on epithelium and mesenchyme in mouse embryonic lung. Dev Biol. 2006; 293:77–89. [PubMed: 16494859]

Dudley AT, Godin RE, Robertson EJ. Interaction between FGF and BMP signaling pathways regulates development of metanephric mesenchyme. Genes Dev. 1999; 13:1601–1613. [PubMed: 10385628]

Dudley AT, Lyons KM, Robertson EJ. A requirement for bone morphogenetic protein-7 during development of the mammalian kidney and eye. Genes Dev. 1995; 9:2795–2807. [PubMed: 7590254]

Dudley AT, Robertson EJ. Overlapping expression domains of bone morphogenetic protein family members potentially account for limited tissue defects in BMP7 deficient embryos. Dev Dyn. 1997; 208:349–362. [PubMed: 9056639]

Fuchs E. Skin stem cells: rising to the surface. J Cell Biol. 2008

Fujimura S, Jiang Q, Kobayashi C, Nishinakamura R. Notch2 Activation in the Embryonic Kidney Depletes Nephron Progenitors. J Am Soc Nephrol. 2010

Godin RE, Takaesu NT, Robertson EJ, Dudley AT. Regulation of BMP7 expression during kidney development. Development. 1998; 125:3473–3482. [PubMed: 9693150]

Grieshammer U, Cebrian C, Ilagan R, Meyers E, Herzlinger D, Martin GR. FGF8 is required for cell survival at distinct stages of nephrogenesis and for regulation of gene expression in nascent nephrons. Development. 2005

Hartman HA, Lai HL, Patterson LT. Cessation of renal morphogenesis in mice. Dev Biol. 2007; 310:379–387. [PubMed: 17826763]

Herzlinger D, Qiao J, Cohen D, Ramakrishna N, Brown AM. Induction of kidney epithelial morphogenesis by cells expressing Wnt-1. Dev Biol. 1994; 166:815–818. [PubMed: 7813799]

Huh SH, Jones J, Warchol ME, Ornitz DM. Differentiation of the lateral compartment of the cochlea requires a temporally restricted FGF20 signal. PLoS Biol. 2012; 10:e1001231. [PubMed: 22235191]

Humphreys BD, Valerius MT, Kobayashi A, Mugford JW, Soeung S, Duffield JS, McMahon AP, Bonventre JV. Intrinsic Epithelial Cells Repair the Kidney after Injury. Cell Stem Cell. 2008 in press.

Itoh N, Ornitz DM. Fibroblast growth factors: from molecular evolution to roles in development, metabolism and disease. J Biochem. 2011; 149:121–130. [PubMed: 20940169]

Karner CM, Das A, Ma Z, Self M, Chen C, Lum L, Oliver G, Carroll TJ. Canonical Wnt9b signaling balances progenitor cell expansion and differentiation during kidney development. Development. 2011

Keller G, Zimmer G, Mall G, Ritz E, Amann K. Nephron Number in Patients with Primary Hypertension. N Engl J Med. 2003; 348:101–108. [PubMed: 12519920]

Kispert A, Vainio S, McMahon AP. Wnt-4 is a mesenchymal signal for epithelial transformation of metanephric mesenchyme in the developing kidney. Development. 1998; 125:4225–4234. [PubMed: 9753677]

Kobayashi A, Valerius MT, Mugford JW, Carroll TJ, Self M, Oliver G, McMahon AP. Six2 defines and regulates a multipotent self-renewing nephron progenitor population throughout mammalian kidney development. Cell Stem Cell. 2008; 3:169–181. [PubMed: 18682239]

Li H, Durbin R. Fast and accurate long-read alignment with Burrows-Wheeler transform. Bioinformatics. 2010; 26:589–595. [PubMed: 20080505]

Li J, Chen F, Epstein JA. Neural crest expression of Cre recombinase directed by the proximal Pax3 promoter in transgenic mice. Genesis. 2000; 26:162–164. [PubMed: 10686619]

Li L, Clevers H. Coexistence of quiescent and active adult stem cells in mammals. Science. 2010; 327:542–545. [PubMed: 20110496]

Lin Y, Liu G, Wang F. Generation of an Fgf9 conditional null allele. Genesis. 2006; 44:150–154. [PubMed: 16496342]

Little MH, Bertram JF. Is there such a thing as a renal stem cell? J Am Soc Nephrol. 2009; 20:2112–2117. [PubMed: 19713310]

Little MH, Brennan J, Georgas K, Davies JA, Davidson DR, Baldock RA, Beverdam A, Bertram JF, Capel B, Chiu HS, et al. A high-resolution anatomical ontology of the developing murine genitourinary tract. Gene Expr Patterns. 2007; 7:680–699. [PubMed: 17452023]

Lusis M, Li J, Ineson J, Christensen ME, Rice A, Little MH. Isolation of clonogenic, long-term self renewing embryonic renal stem cells. Stem Cell Res. 2010; 5:23–39. [PubMed: 20434421]

McMahon AP, Aronow BJ, Davidson DR, Davies JA, Gaido KW, Grimmond S, Lessard JL, Little MH, Potter SS, Wilder EL, et al. GUDMAP: the genitourinary developmental molecular anatomy project. J Am Soc Nephrol. 2008; 19:667–671. [PubMed: 18287559]

Michos O, Cebrian C, Hyink D, Grieshammer U, Williams L, D'Agati V, Licht JD, Martin GR, Costantini F. Kidney development in the absence of Gdnf and Spry1 requires Fgf10. PLoS Genet. 2010; 6:e1000809. [PubMed: 20084103]

Myrie SB, McKnight LL, Van Vliet BN, Bertolo RF. Low Birth Weight Is Associated with Reduced Nephron Number and Increased Blood Pressure in Adulthood in a Novel Spontaneous Intrauterine Growth-Restricted Model in Yucatan Miniature Swine. Neonatology. 2011; 100:380–386. [PubMed: 21791929]

Ornitz DM, Xu J, colvin JS, McEwen DG, MacArthur CA, Coulier F, Gao G, Goldfarb M. Receptor specificity of the fibroblast growth factor family. Journal of Biological Chemistry. 1996; 271:15292–15297. [PubMed: 8663044]

Osafune K, Takasato M, Kispert A, Asashima M, Nishinakamura R. Identification of multipotent progenitors in the embryonic mouse kidney by a novel colony-forming assay. Development. 2006; 133:151–161. [PubMed: 16319116]

Park JS, Valerius MT, McMahon AP. Wnt/{beta}-catenin signaling regulates nephron induction during mouse kidney development. Development. 2007; 134:2533–2539. [PubMed: 17537789]

Perantoni AO, Dove LF, Karavanova I. Basic fibroblast growth factor can mediate the early inductive events in renal development. Proc Natl Acad Sci U S A. 1995; 92:4696–4700. [PubMed: 7753867]

Perantoni AO, Timofeeva O, Naillat F, Richman C, Pajni-Underwood S, Wilson C, Vainio S, Dove LF, Lewandoski M. Inactivation of FGF8 in early mesoderm reveals an essential role in kidney development. Development. 2005

Poladia DP, Kish K, Kutay B, Hains D, Kegg H, Zhao H, Bates CM. Role of fibroblast growth factor receptors 1 and 2 in the metanephric mesenchyme. Dev Biol. 2006; 291:325–339. [PubMed: 16442091]

Qiao J, Uzzo R, Obara-Ishihara T, Degenstein L, Fuchs E, Herzlinger D. FGF-7 modulates ureteric bud growth and nephron number in the developing kidney. Development. 1999; 126:547–554. [PubMed: 9876183]

Sakaki-Yumoto M, Kobayashi C, Sato A, Fujimura S, Matsumoto Y, Takasato M, Kodama T, Aburatani H, Asashima M, Yoshida N, et al. The murine homolog of SALL4, a causative gene in Okihiro syndrome, is essential for embryonic stem cell proliferation, and cooperates with Sall1 in anorectal, heart, brain and kidney development. Development. 2006; 133:3005–3013. [PubMed: 16790473]

Saxen L, Lehtonen E. Embryonic kidney in organ culture. Differentiation. 1987; 36:2–11. [PubMed: 3328727]

Saxen L, Sariola H. Early organogenesis of the kidney. Pediatr Nephrol. 1987; 1:385–392. [PubMed: 3153305]

Self M, Lagutin OV, Bowling B, Hendrix J, Cai Y, Dressler RD, Oliver G. Six2 is required for suppression of nephrogenesis and progenitor renewal in the developing kidney. Embo J. 2006; 25:5214–5228. [PubMed: 17036046]

Sims-Lucas S, Cusack B, Baust J, Eswarakumar VP, Masatoshi H, Takeuchi A, Bates CM. Fgfr1 and the IIIc isoform of Fgfr2 play critical roles in the metanephric mesenchyme mediating early inductive events in kidney development. Dev Dyn. 2011; 240:240–249. [PubMed: 21128305]

Stratman JL, Barnes WM, Simon TC. Universal PCR genotyping assay that achieves single copy sensitivity with any primer pair. Transgenic Res. 2003; 12:521–522. [PubMed: 12885173]

White AC, Xu J, Yin Y, Smith C, Schmid G, Ornitz DM. FGF9 and SHH signaling coordinate lung growth and development through regulation of distinct mesenchymal domains. Development. 2006; 133:1507–1517. [PubMed: 16540513]

Yayon A, Klagsbrun M, Esko JD, Leder P, Ornitz DM. Cell surface, heparin-like molecules are required for binding of basic fibroblast growth factor to its high affinity receptor. Cell. 1991; 64:841–848. [PubMed: 1847668]

Yin Y, Wang F, Ornitz DM. Mesothelial- and epithelial-derived FGF9 have distinct functions in the regulation of lung development. Development. 2011; 138:3169–3177. [PubMed: 21750028]

Yin Y, White AC, Huh SH, Hilton MJ, Kanazawa H, Long F, Ornitz DM. An FGF-WNT gene regulatory network controls lung mesenchyme development. Dev Biol. 2008; 319:426–436. [PubMed: 18533146]

Yu J, Carroll TJ, McMahon AP. Sonic hedgehog regulates proliferation and differentiation of mesenchymal cells in the mouse metanephric kidney. Development. 2002; 129:5301–5312. [PubMed: 12399320]

Zhang X, Ibrahimi OA, Olsen SK, Umemori H, Mohammadi M, Ornitz DM. Receptor specificity of the fibroblast growth factor family. The complete mammalian FGF family. J Biol Chem. 2006; 281:15694–15700. [PubMed: 16597617]

Zhou M, Sutliff RL, Paul RJ, Lorenz JN, Hoying JB, Haudenschild CC, Yin M, Coffin JD, Kong L, Kranias EG, et al. Fibroblast growth factor 2 control of vascular tone. Nat Med. 1998; 4:201–207. [PubMed: 9461194]

Highlights

- FGF20 and FGF9 are the niche ligands for developing metanephric kidney progenitors
- FGF9 is expressed in duct epithelia, both ligands are expressed by progenitor cells
- FGF20 loss in humans, or FGF9/20 loss in mice, results in kidney agenesis
- FGF9/20 can maintain competence of sorted, pure progenitor cell populations in vitro

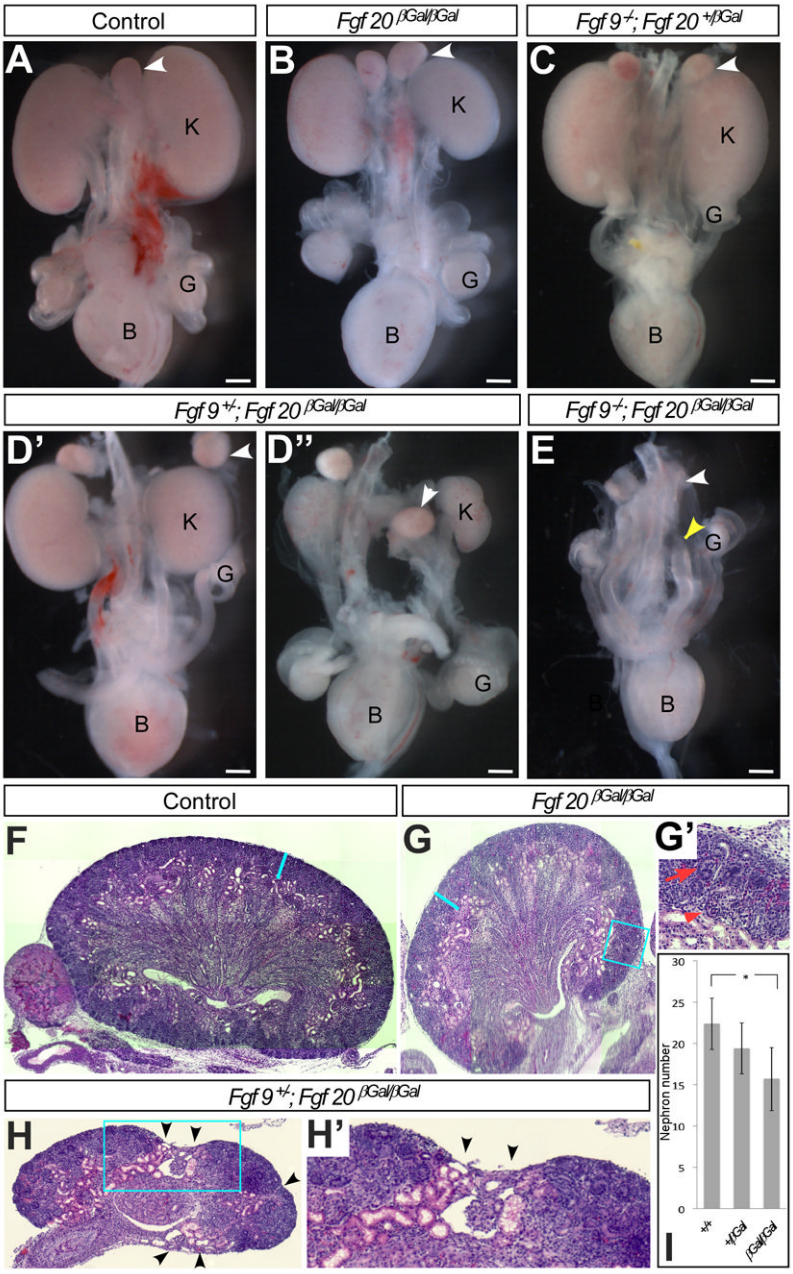

Figure 1. *Fgf20* and *Fgf9* are required for kidney development

A-C) Normal urogenital system formed in control (A), *Fgf20*$^{\beta Gal/\beta Gal}$ (B) and *Fgf9*$^{+/-}$ *Fgf20*$^{+/\beta Gal}$ (C) embryos. Note slightly smaller kidneys in (B) but not in (C). D) *Fgf9*$^{+/-}$; *Fgf20*$^{\beta Gal/\beta Gal}$ embryos developed mild (D') to severe (D") reduction in kidney size. E) When both alleles were deleted the kidneys were absent (yellow arrowhead) and adrenal glands were smaller (white arrowhead). F,G) H&E staining of kidneys from control (F) and *Fgf20*$^{\beta Gal/\beta Gal}$ (G) mice shows bilateral reduction in kidney size of mutant compared to control. Nephrogenic zone thickness (white line) is indistinguishable between *Fgf20*$^{\beta Gal/\beta Gal}$ and control kidneys. High power image of boxed area in G shows normal intermediate steps in nephron development (SSB, arrow; early glomeruli, arrowhead in G'). H) Kidney section of *Fgf9*$^{+/-}$; *Fgf20*$^{\beta Gal/\beta Gal}$ embryo showed regions where the nephrogenic zone was depleted

(arrowheads). H') High power image of boxed area in H. Glomeruli were counted from 4 control, 5 *Fgf20*$^{+/\beta Gal}$ and 5 *Fgf20*$^{\beta Gal/\beta Gal}$ kidneys. Average count (in thousands with S.D) is shown in (I). Asterisk p= 8.1775×10^{-8}. Kidney (K), Gonad (G) and Bladder (B). Scale bar: 500μm.

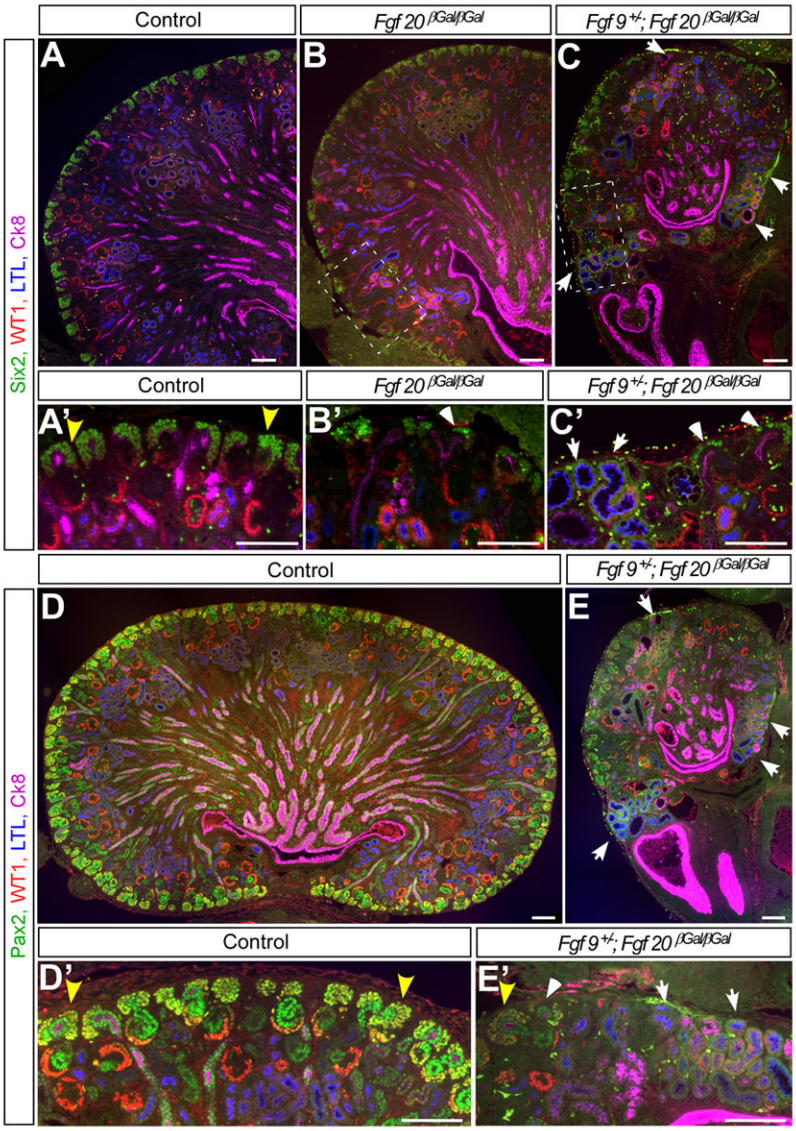

Figure 2. Loss of nephron progenitors in *Fgf9/20* mutants

Sections of E18.5 kidneys stained with Ck8 (purple, UB), WT1 (Red; low, CMM; high, podocytes), LTL (blue, proximal tubules), Six2 (green, progenitors) or Pax2 (UB, nephron progenitors and nephron epithelia). (A, D). The nephrogenic zone in controls (green) is located distal to the UB and to glomeruli (red) attached to proximal tubules (blue). A'-D') High power image of control nephrogenic zone showed progenitors (yellow arrowheads) packed in two compact cell layers distal UB tips. B) The nephrogenic zone near some tips in $Fgf20^{\beta Gal/\beta Gal}$ kidneys contains fewer Six2+ cells relative to controls but is otherwise indistinguishable (high power view in B'). C-E) $Fgf9^{+/-}; Fgf20^{\beta Gal/\beta Gal}$ kidneys contained many cortical areas where the nephrogenic zone was replaced by mature structures (white arrows). C'-E') High power image of nephrogenic zone from $Fgf9^{+/-}; Fgf20^{\beta Gal/\beta Gal}$ kidneys. The cortex contained some UB tips surrounded by two cell layers of nephron progenitors (yellow arrowheads), other tips with fewer Six2+ cells (white arrowheads), and some lacking a nephrogenic zone altogether contained mature nephrons instead (white arrows). Scale bars: 100μm.

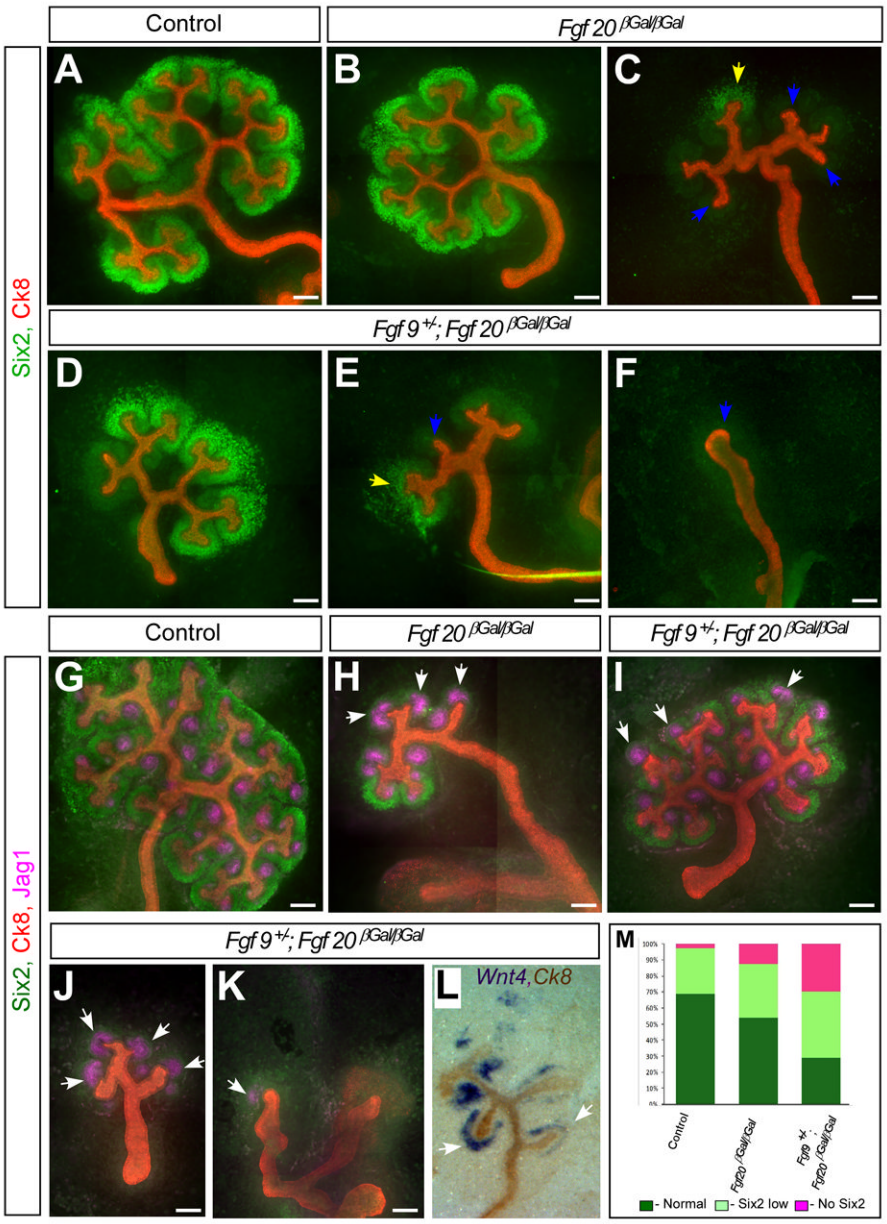

Figure 3. Reduced *Fgf9/20* levels allow premature differentiation of nephron progenitors in the niche

E11.5 metanephroi analyzed after 48hrs in organ culture (A-F). *Fgf20*$^{\beta Gal/\beta Gal}$ metanephroi (B,C) were smaller than controls (A). B-F) Some UB tips in *Fgf20*$^{\beta Gal/\beta Gal}$ metanephroi (B-C) or *Fgf9*$^{+/-}$*; Fgf20*$^{\beta Gal/\beta Gal}$ metanephroi (D-F) are surrounded by fewer Six2+ cells (yellow arrow), while others lack Six2 expressing cells (blue arrows). G-K) Jag1 (epithelial RVs and SSBs), Ck8 (UB), and Six2 (nephron progenitors) demonstrate premature differentiation in the niche in metanephroi distal to some UB tips (white arrows). L) *In situ* hybridization of *Wnt4* (blue) and antibody staining to Ck8 (brown) shows ectopic *Wnt4* expression distal to UB tips in *Fgf9*$^{+/-}$*; Fgf20*$^{\beta Gal/\beta Gal}$ metanephroi (white arrows). M) Quantification of tip subtypes (marked with yellow or blue arrows) in metanephroi of various genotypes (supplemental information). Normal progenitor numbers in dark green reduced progenitors numbers in light green; no progenitors in pink. Scale bars: 100μm.

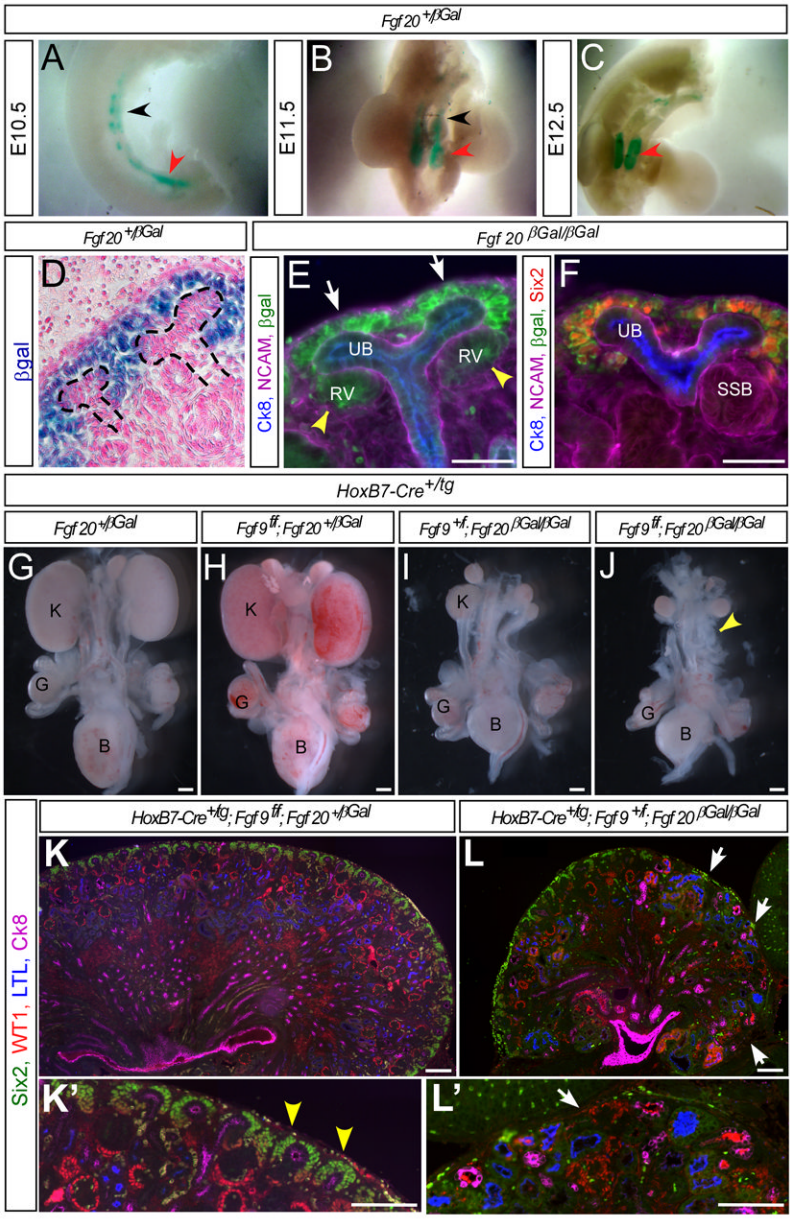

Figure 4. *Fgf20* expressed in nephron progenitors and *Fgf9* secreted from the UB collaborate to maintain the niche

A-C) Whole-mount x-gal staining at E10.5-12.5 *Fgf20*$^{\beta Gal}$ embryos detects ßGal activity (blue) in the mesonephros (black arrowheads) and metanephric kidneys (red arrowheads). D) X-gal staining identified activity in the MM of E14.5 *Fgf20*$^{\beta Gal}$ kidneys (black dashed line-UB). E) Ck8, NCAM (epithelia) and ßGal (*Fgf20* expression domain) staining of E16.5 *Fgf20*$^{\beta Gal/\beta Gal}$ kidneys. ßGal protein was detected in the CMM (white arrows). The weak signal in the nascent RV (yellow arrowheads) may be due to expression or perdurance. F) Six2 identified nephron progenitors that contained ßGal protein. G-J) Urogenital system in mice lacking *Fgf9* in their UB. G) Control (*HoxB7-Cre*$^{+/tg}$;*Fgf20*$^{+/\beta Gal}$; H) and *HoxB7-Cre*$^{+/tg}$;*Fgf9*$^{f/f}$;*Fgf20*$^{+/\beta Gal}$ kidneys appeared normal. I) In contrast, *HoxB7-Cre*$^{+/tg}$;*Fgf9*$^{+/f}$;*Fgf20*$^{\beta Gal/\beta Gal}$ kidneys are smaller. J) Fully penetrant kidney agenesis (yellow arrowhead) seen in *HoxB7-cre;Fgf9*$^{f/f}$; *Fgf20*$^{\beta Gal/\beta Gal}$ embryos. K-L) Ck8

(magenta), WT1 (red), LTL (blue) and Six2 (green) staining of *HoxB7-Cre*^{tg}; *Fgf9*$^{f/f}$; *Fgf20*$^{+/\beta Gal}$ (control, K) or *HoxB7-Cre*^{tg}; *Fgf9*$^{+/f}$; *Fgf20*$^{\beta Gal/\beta Gal}$ (L) kidneys. Note large cortical areas where the nephrogenic zone was replaced by mature structures (white arrows, L). High power image of nephrogenic zone of control *HoxB7-Cre*^{tg}; *Fgf9*$^{f/f}$; *Fgf20*$^{+/\beta Gal}$ kidney (K', yellow arrowheads) or *HoxB7-Cre*^{tg}; *Fgf9*$^{+/f}$; *Fgf20*$^{\beta Gal/\beta Gal}$ kidney (L'). Note regions lacking Six2 with mature structures (podocytes: red; proximal tubules: blue) located instead at edge of kidney (white arrows). Kidney (K), Gonad (G), Bladder (B). Scale bars: 50μm (E-F), 500μm (G-J), 100μm (K-L').

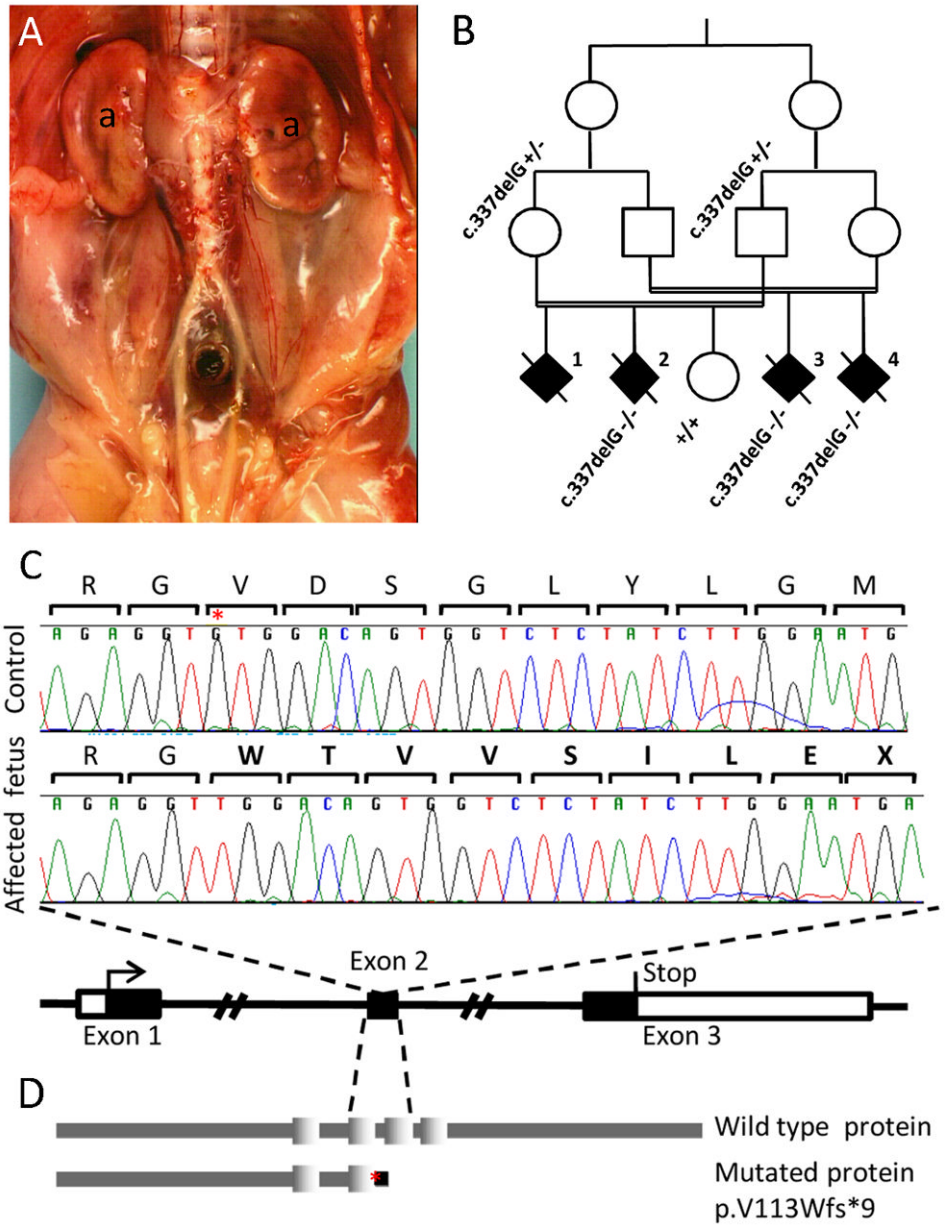

Figure 5. Identification of a homozygous frameshift mutation in FGF20 that segregates with bilateral renal agenesis

(A) Bilateral reno-ureteral agenesis in 18-week fetus; (a) adrenal glands with flat oval shape due to kidney agenesis. (B) Pedigree of the consanguineous family showing two first cousin couples and four fetuses presenting with anhydramnios / bilateral renal agenesis; segregation of the FGF20 c.337delG mutation is indicated. (C) Nucleotide sequence traces and deduced amino acid sequence within exon 2 shown for wild type (top) and mutated (bottom) alleles. Deleted guanine at position 337 of the coding sequence is marked with asterisk in the wild type sequence. The frameshift introduced missense amino acids from position 113 to 120 (in bold) and created a stop codon at position 121 (numbering as in NCBI sequence AB030648). (D) Wild type and deduced FGF20 proteins: Heparin-binding domains indicated by light grey boxes; position of mutation is marked with red asterisk; the 8 missense amino acids are in black.

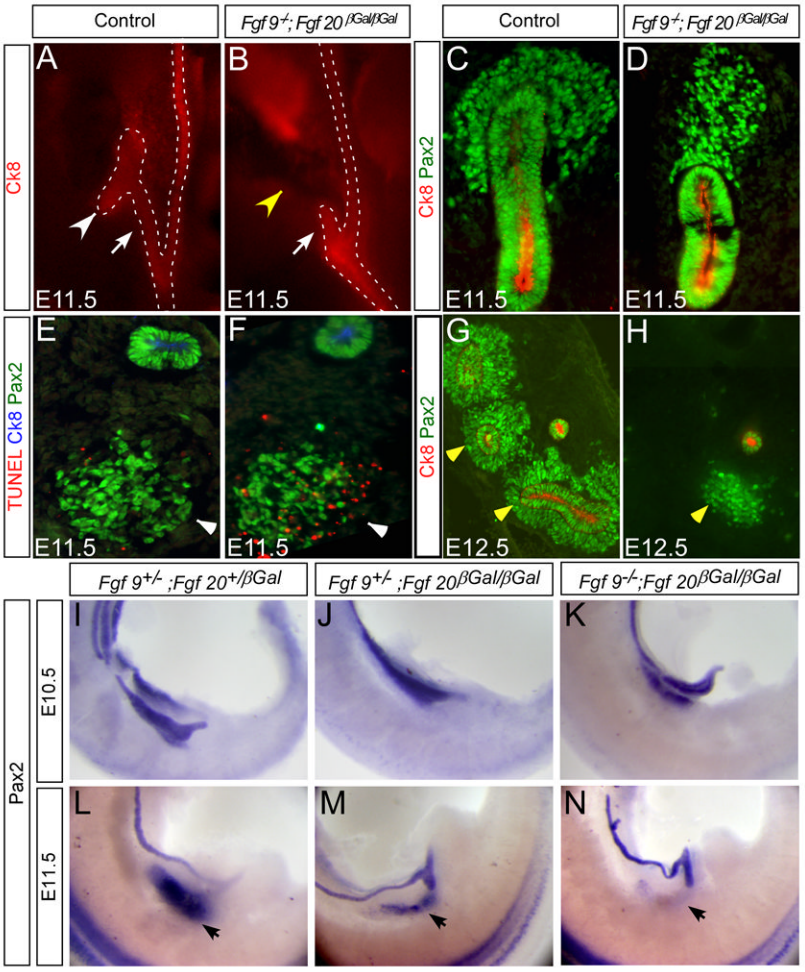

Figure 6. ***Fgf9/20*** **deficient kidneys initiate UB outgrowth but branching fails due to high rates of apoptosis in the MM**

E11.5 whole-mount Ck8 staining in controls (A) illustrated a branched UB (white arrowhead). In contrast, the UB in *Fgf9*$^{-/-}$; *Fgf20*$^{\beta Gal/\beta Gal}$ E11.5 embryos (B) elongated (arrow) but failed to branch (yellow arrowhead). Sections of E11.5 kidneys stained with Pax2 (UB and MM) showed MM condensing around the UB tips (Ck8+) in controls (C) but not in *Fgf9*$^{-/-}$; *Fgf20*$^{\beta Gal/\beta Gal}$ embryos (D). The mutant MM appeared diffuse and formed a smaller contact zone with the UB. MM in control is Pax2 positive and TUNEL negative (E); the dying MM cells in *Fgf9*$^{-/-}$; *Fgf20*$^{\beta Gal/\beta Gal}$ embryos are TUNEL positive (white arrowheads in F). At E12.5, Ck8 and Pax2 outline a rudimentary MM remaining in *Fgf9*$^{-/-}$; *Fgf20*$^{\beta Gal/\beta Gal}$ embryos (H) compared to controls (G) (yellow arrowheads in G-H).

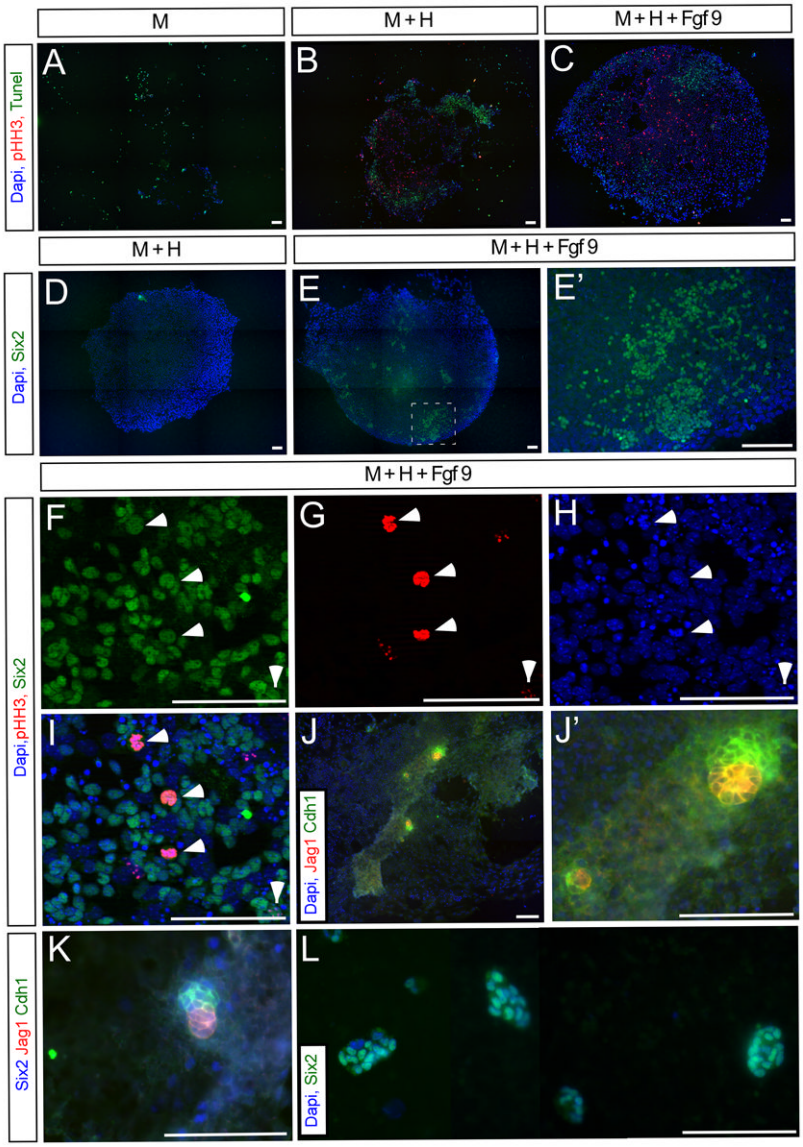

Figure 7. Fgf9 promotes survival and maintains competence of nephron progenitors *in vitro*

Isolated E11.5 MM cultured in defined media (M; A), in Heparin-supplemented media (M +H; B), or in Heparin and Fgf9 media (M+H+Fgf9; C,E-K). Explants were fixed and stained as indicated. After 4 days in media, the majority of MM cells were TUNEL-positive (A). When supplemented with Heparin, cell survival improved, some entering mitosis (B). In the presence of Fgf9, survival and proliferation were further increased (C). Isolated E11.5 MM was grown in culture for 2 days with M+H (D) or M+H+Fgf9 (E-I). Six2+ cells were only detected when Fgf9 was present (E, E'). A few progenitors (left-pointing arrowheads) positive for Six2 (F), pHH3 (G) and DAPI (H) underwent mitosis (merged image; I). Nephron progenitors maintained in the presence of Fgf9 for 2 days are competent to respond to Wnt produced by dSC by forming epithelial aggregates expressing both distal (Cdh1+) and proximal (Jag1+) markers (J, J', higher magnification; see text for detail). Note undifferentiated, Six2+ cells in (K). Colonies of Six2+ cells isolated by FACS were maintained for 2 days in culture in M+H+Fgf9 (L). Scale bars: 100μm.

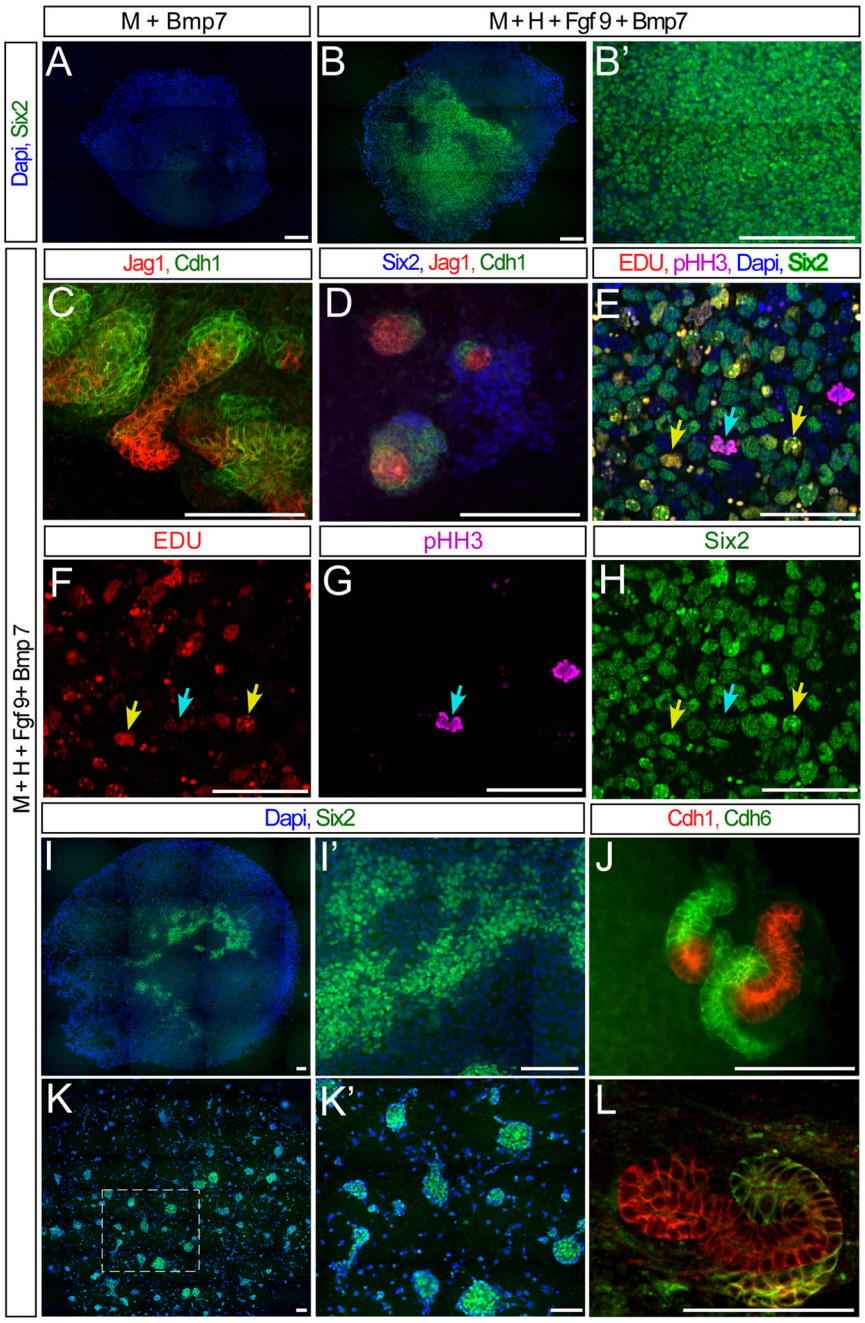

Figure 8. Fgf9 synergized with Bmp7 to promote self-renewal of competent nephron progenitors *in vitro*

Isolated E11.5 MM was grown for 48hrs in media supplemented with Bmp7 (A) or Heparin with Fgf9 and Bmp7 (M+H+Fgf9+Bmp7) (B-J). Six2+ cells were not detected in explants grown with Bmp7 (A). In explants cultured in M+H+Fgf9+Bmp7, many Six2+ cells are detected (B-B'). Note that Six2+ cells sorted into a tight cluster with a clear boundary separating them from Six2− cells (B). Adding dSC to cells pretreated by M+H+Fgf9+Bmp7 induced robust differentiation (C). Epithelial aggregates (Cdh1+, Jag+) are surrounded by Six2+ cells (D). Isolated E11.5 MM cultured in M+H+Fgf9+Bmp7 media and EdU (5-ethynyl-2'-deoxyuridine) for 4-7hr, washed and cultured in M+H+Fgf9+Bmp7 for

additional 44hrs. Explants were stained with EdU detection kit (E-F), pHH3 (E, G) and Six2 (E, H) Many Six2+ cells remained EDU^{bright} (E-H, yellow arrows), suggesting that they did not divide again within 48hr. A few nephron progenitors Six2+, EDU^{Dimm} (cells that divided once after labeling), pHH3+ cells were able to divide at least once within two days of culture. Isolated E11.5 MM was grown for 5 days in M+H+Fgf9+Bmp7. Many Six2+ nephron progenitors survived (I, a close-up in I'). Adding dSC after 5 days induced robust epithelial differentiation of either distal (Cdh1+) or proximal (Cdh6+) character (J). *Six2-GFP* expressing cells were sorted, cultured with M+H+Fgf9+Bmp7 and stained for Six2 after 48hrs (K, close-up in K'). Adding dSC to these cells for an additional 4 day period induced differentiation of distal (Cdh1+) or proximal (Cdh6+) epithelia (L). Scale bars: 100μm.